
Mining the Local Volume

Igor D. Karachentsev¹, Valentina Karachentseva², Walter Huchtmeier³,
Dmitry Makarov¹, Serafim Kaisin¹, Margarita Sharina¹, and Lidia
Makarova¹

¹ Special Astrophysical Observatory, Russian Academy of Sciences, N. Arkhyz,
369167, Russia

ikar@sao.ru, dim@sao.ru, skai@sao.ru, sme@sao.ru, lidia@sao.ru

² Astronomical Observatory, Kiev National University, Kiev, 04053 Ukraine
vkarach@observ.univ.kiev.ua

³ Max-Planck-Institut für Radioastronomie, Auf dem Hügel 69, D-53121 Bonn,
Germany p083huc@mpifr-bonn.de

Absrtact.

After recent systematic optical, IR, and HI surveys, the total number of known galaxies within 10 Mpc has increased from 179 to 550. About half this Local Volume (LV) sample is now been imaged with HST, yielding the galaxy distances with an accuracy of about 8%. For the majority of the LV galaxies we currently have H α fluxes that allow us to reconstruct the star formation history of our neighbourhood.

For the late-type LV galaxies their HI masses and angular momentum follow the linear relation in the range of 4 orders, which is expected for rotating gaseous disks being near the gravitational instability threshold.

The data obtained on the LV galaxies imply important cosmological parameters, in particular, the mean local matter density and HI mass density, as well as SFR density.

Surprisingly, the local Hubble flow around the LV groups is very quiet, with 1D rms deviations of 25 km s⁻¹, which is a signature of the Universe vacuum-dominated on small scales. The cold infall pattern around nearby groups provides us with a new method to determine the total mass of the groups independent from virial mass estimates.

1 The Local volume census.

The first step towards compiling a Local volume (LV) sample of galaxies situated within 10 Mpc was made by Kraan-Korteweg & Tammann [1] who published a list of 179 nearby galaxies with radial velocities $V_{LG} < 500$ km s⁻¹. Then Karachentsev [2] updated their list to 226 objects. Later, fast increasing the LV sample was proceeding by different ways: a) via Z-surveys of the known (UGC, MCG, CGCG) catalogues; b) based on special searches for dwarf

members of nearby groups around M 31, M 81, IC 342, Cen A, NGC 253, M 94, M 101, NGC 6946; c) from searches for LSB galaxies in wide sky regions; d) via special HI and NIR surveys in the Zone of Avoidance; e) from blind HI sky surveys (Staveley-Smith et al.[3], Koribalski et al. [4]).

During the last decade, a comprehensive study of the LV galaxies was undertaken by Karachentseva & Karachentsev and their co-workers. The basic steps of this long-term project are listed in Table 1.

Table 1. Basic stages of the project

Item	Means	Status	Results
All-sky search for new Local volume members.	POSS-II, ESO/SERC.	100%	350 new LSB dwarf galaxies were found.
HI line survey of 600 dwarfs from KK-lists.	Effelsberg, Nancey, ATCA.	100%	100 new LV dwarfs with $V_{LG} < 550 \text{ km s}^{-1}$.
CCD (B,V,R)- imaging of the LV galaxies.	6m SAO, 2.5m Nordic.	50%	150 LV members resolved into stars for the first time.
Distance measurements to the LV galaxies.	HST.	50%	accurate TRGB distances to 200 galaxies.
$H\alpha$ imaging all the LV galaxies.	6m SAO, 2.2m ESO.	60%	HII-pattern and SFR for 300 galaxies.
HI velocity field for 90 tiny dIrrs [5].	GMRT	80%	Dark Matter properties on scales of ~ 1 kpc.

General observational data on 451 galaxies were summarized in the Catalog of Neighboring Galaxies by Karachentsev et al. [6]. The present version of the LV sample contains 550 objects.

As it is known, the simpler selection criterion taken for any sample, the easier interpretation of the sample properties. This Heisenberg's principle of (un)certainly gives a great advantage to the LV sample because of its simplest selection criterion, $D < 10$ Mpc.

However, an improving census of the Local Volume has a two-way traffic. Modern automated redshift surveys, like SDSS, 2dF, DEEP2, 6dF, produce a lot of spurious objects with radial velocities around zero. For instance, the DEEP2 survey generated about 700 false members of the LV fixed in LEDA and NED. There are also some cases in these databases, like "dIrr galaxy" AM 0912-241 with $V_h = +614 \text{ km s}^{-1}$ which turns out to be a photographic emulsion defect.

2 Mapping galaxy distribution and peculiar velocities in the LV.

The sky distribution of the LV galaxies looks extremely inhomogeneous owing to the presence of galaxy groups [7] and voids [8]. Spatial distribution of the nearest galaxies inside and around the Local group (LG) is presented in Fig. 1 in the Supergalactic coordinates. Galaxies of different linear diameters are shown by different size balls. The circle indicates the radius of zero-velocity surface ($R_o = 0.9$ Mpc) separating the LG against the cosmic Hubble expansion. The edge-on view of the LG and its suburbs (lower panel) demonstrates larger scatter of dwarf galaxies with respect to the SG plane.

While having accurate velocities and distances for 200 LV galaxies, one can study distribution of peculiar velocities within the LV. Fig. 2 presents a peculiar velocity map for the LV galaxies in the equatorial coordinates given in the LG reference frame and smoothed with a window of 15° . The distribution shows the local Hubble flow to be generally quiet (± 30 km s $^{-1}$) with a small area of negative peculiar velocities -250 km s $^{-1}$ in the direction towards the Leo constellation. This phenomena can be caused by the apparent motion of the Local Sheet as a whole from the large Local void towards the neighboring Leo cloud [9]. Note that the local peculiar velocity field observed on a scale of 10 Mpc has not any relation to the so-called Virgo-centric infall often used by different authors to "improve" distances to nearby galaxies via their velocities.

3 Some basic relations for the LV galaxies.

Besides the global (external) Hubble law, galaxies follow another internal "Hubble law-2", the linear relation between their rotation velocity and standard radius:

$$V = h \cdot R,$$

where $h = 137H_0$, or $1/h = 100$ Myr. This leads to the known empirical relations between total mass M_t , luminosity L , total angular momentum J , and surface brightness SB of a galaxy:

$$M_t \propto L \propto R \cdot V^2 \propto R^3,$$

meaning that the average spatial densities of giant, normal, and dwarf galaxies are almost the same;

$$L \propto V^3,$$

corresponding on a logarithmic scale to the Tully-Fisher relation;

$$J \propto M \cdot V \cdot R \propto M^{5/3},$$

which is known as Muradyan law valid for a much wider range of celestial bodies from asteroids to galaxy superclusters [10];

$$SB \propto L/R^2 \propto R,$$

Binggeli-Grebel relation (valid also for E and dSph galaxies), which makes one search for extremely faint dwarf galaxies among the objects of the lowest

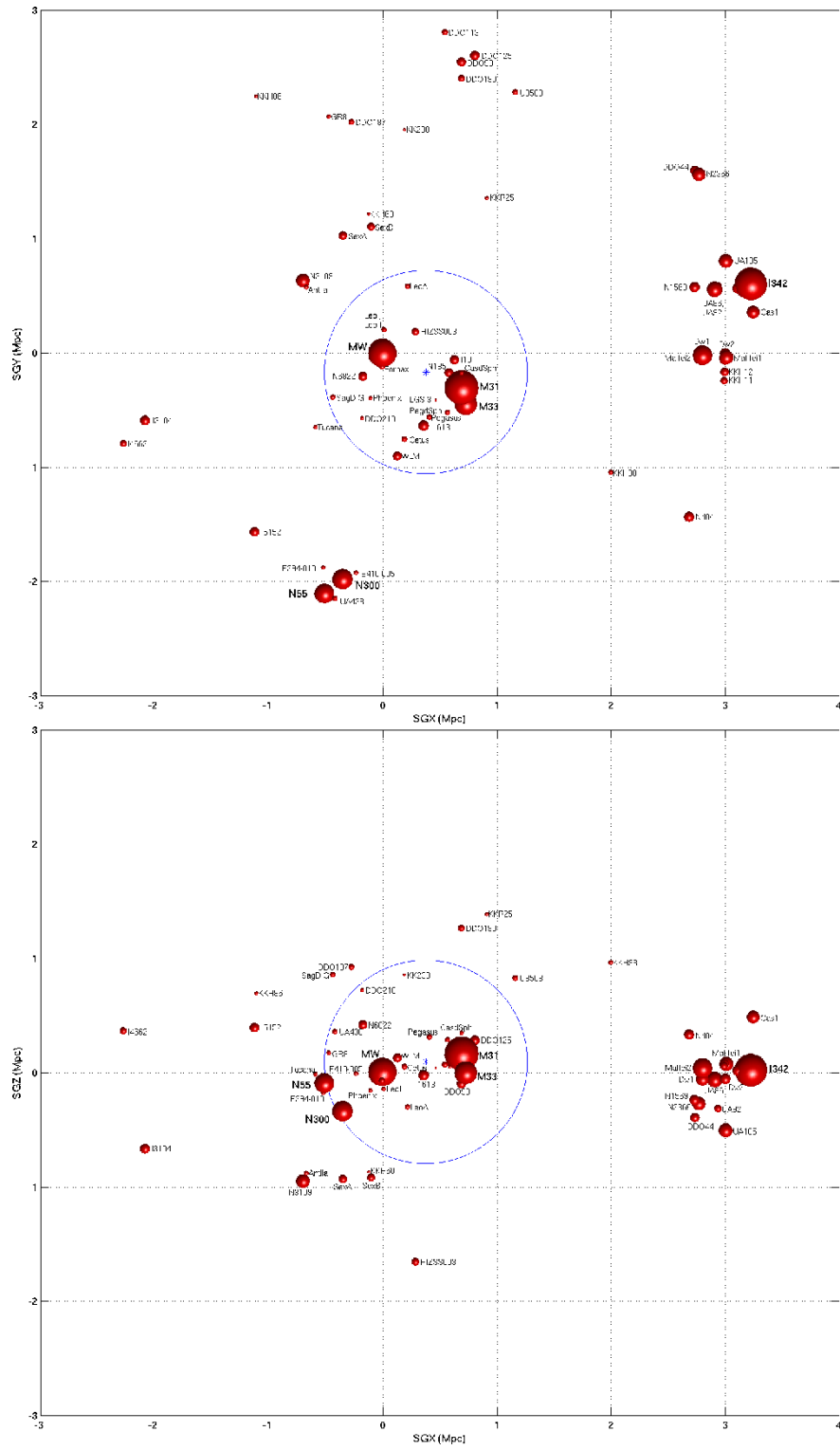


Fig. 1. Spatial distribution of the nearest galaxies inside and around the Local group in the Supergalactic coordinates

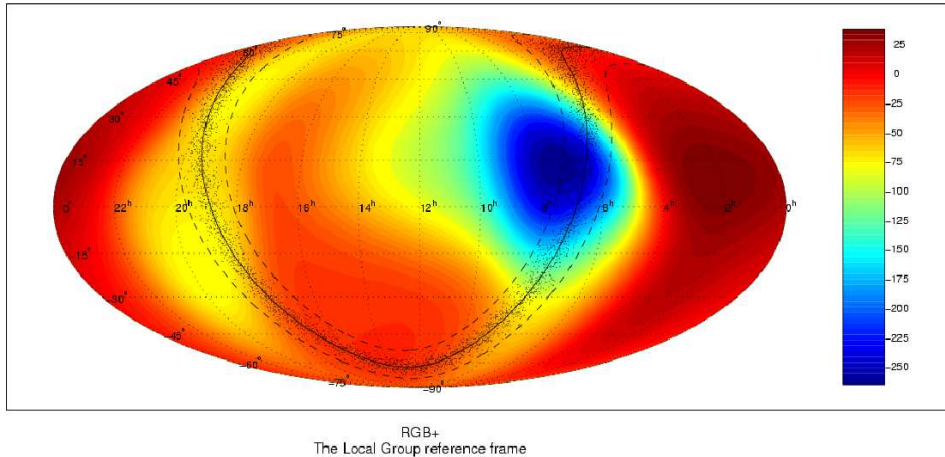


Fig. 2. Peculiar velocity map for the LV galaxies

surface brightness. These empirical scaling relations probably mean that stellar population of dwarf and giant galaxies reside in dark matter "corsets" of a standard profile.

As it was shown by Roberts [11], hydrogen masses of disk-like galaxies follow the empirical relation:

$$M_g \propto R^2,$$

i.e. the mean HI surface brightness of giant and dwarf disks is almost the same. This Roberts law leads to the following scaling relations:

$$M_g/M_t \propto R^2/R^3 \propto 1/R \propto M_t^{-1/3},$$

meaning that dwarf galaxies are relatively more gas-rich systems, being capable of longer star formation activity than giant ones;

$$M_g \propto R \cdot V \propto j,$$

this Zasov relation between total hydrogen mass and specific angular momentum of galaxies, shown in Fig. 3, means that galaxy disks are situated in the state of equilibrium just above the threshold of gravitational instability driving their star formation processes [12].

4 $H\alpha$ flux and SFR for the LV galaxies.

Systematic $H\alpha$ imaging made for the LV galaxies allows us to measure the star formation rate (SFR) for them in an unprecedented wide range. As distinct from other samples, the LV sample offers an unique opportunity to study the SFR for galaxies of different types and in different environment without significant selection biases.

Left and right panels of Fig. 4 present the SFR of nearby galaxies versus their blue absolute magnitude and hydrogen mass, respectively. The dashed

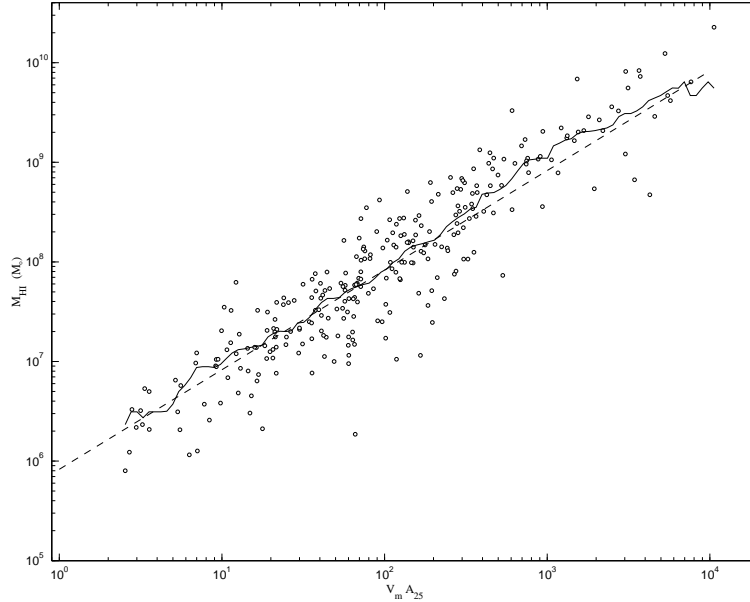


Fig. 3. The total hydrogen mass vs. specific angular momentum of galaxies

lines correspond to a constant SFR per unit luminosity or unit hydrogen mass. As can be seen from the left diagram, most of the galaxies brighter than -13^m follow a linear regression with the constant specific SFR. However, SFRs and hydrogen masses demonstrate a steeper relationship $[SFR] \propto M_{HI}^{3/2}$, shown on the right panel by the solid line. This feature seems to be in harmony with the following considerations noted by Tutukov [13]. According to Schmidt law for local SF sites, their rate of transformation of gas into stars is proportional to the square of gas density:

$$d(n_g)/dt \propto (n_g)^2.$$

Taking into account the above mentioned relations between the galaxy disk parameters, we find that

$$SFR \propto d(n_g)/dt \cdot R^3 \propto (n_g)^2 \cdot R^3 \propto (M_g)^2/R \propto M_g^{3/2},$$

i.e. obtain the known Kennicutt law, but for the galaxies themselves, not for individual HII regions only. Therefore, evolutionary history of disks of galaxies looks to be driven mainly by SF processes.

To characterize the past and the future evolution status of a galaxy, we introduce two dimensionless parameters:

$$p_* = \log [SFR] \cdot T_0/L_B \text{ and } f_* = \log M_{HI}/[SFR] \cdot T_0.$$

The former parameter describes the galaxy formation timescale, the latter shows the gas depletion timescale, both expressed in the Hubble time units, T_0 . The distribution of the LV galaxies on the p_* , f_* -plane is displayed in Fig. 5.

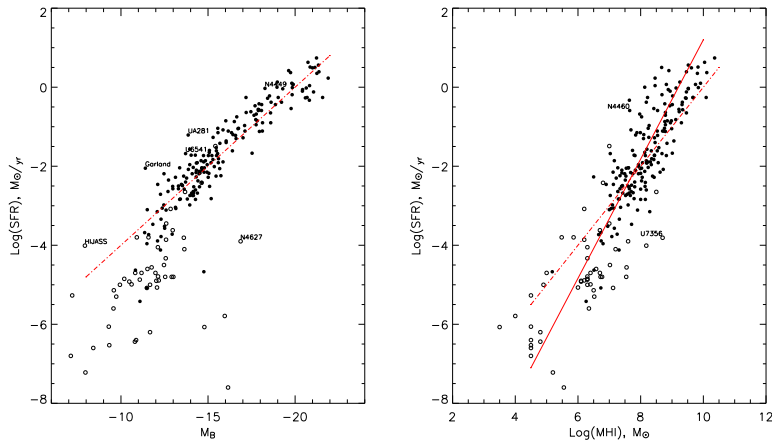


Fig. 4. The SFR of nearby galaxies vs. their blue absolute magnitude (left) and hydrogen mass (right)

As a whole, the LV population concentrates around the origin ($p_* = 0, f_* = 0$) of this diagnostic diagram. It means that the

observed luminosity of a typical LV galaxy may be reproduced with its observed SFR, and a typical LV galaxy has enough gas to continue its observed SFR during the next Hubble time. However, galaxies of different morphological types occupy different regions on the p_*, f_* - diagram that must be a subject of elaborate analysis.

It is generally accepted that the enhanced star formation in galaxies is triggered by their interaction. But we did not find clear evidence for such a suggestion. Curiously, the strongly disturbed tidal dwarf "Garland" near NGC 3077 and the very isolated blue galaxy UGCA 281 have almost the same extremely high specific SFR (see left panel in Fig.4).

5 Basic properties of the nearest groups.

Over the last few years, searches for new nearby dwarf galaxies and accurate distance measurements for them lead to a significant increase of the population of known neighboring groups. Table 2 presents basic parameters of 7 nearest groups situated within 5 Mpc from us: distance to the group centroid, number of the group members with known radial velocities, 1D velocity dispersion, projected radius, crossing time, virial mass, total blue luminosity and virial mass-to-luminosity ratio.

Remarkably, centroids of the groups have the radial velocity dispersion around the local Hubble flow of only 25 km s^{-1} .

Precise measurements of distances and radial velocities for galaxies surrounding a group permits us to determine the radius of zero - velocity surface,

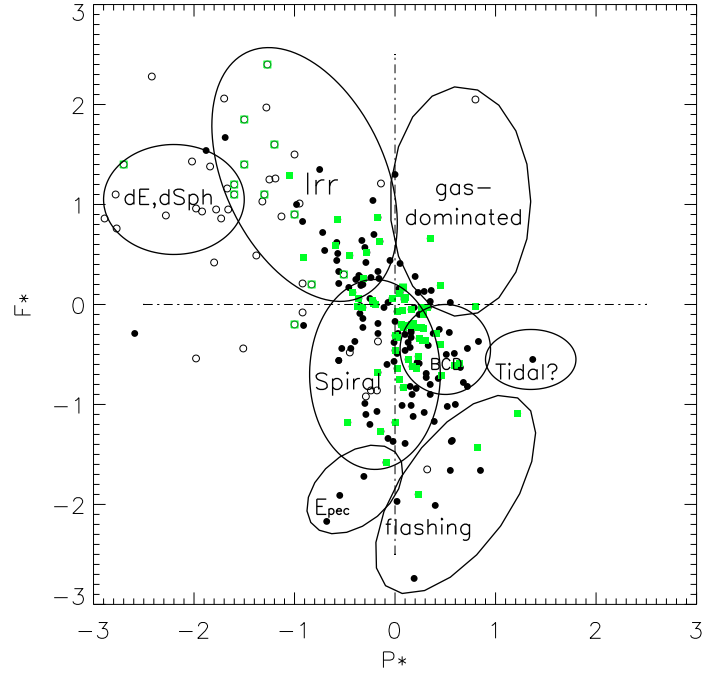


Fig. 5. Distribution of the LV galaxies on the p_* , f_* -plane

Table 2. Basic parameters of the nearest groups

Parameter	M.Way	M31	M81	CenA	M83	IC342	Maffei
D, Mpc	0.01	0.78	3.63	3.66	4.56	3.28	3.01
Nv	18	18	24	29	13	8	8
σ_v , km/s	76	77	91	136	61	54	59
R_p , Mpc	.16	.25	.21	.29	.16	.32	.10
T_{cross} , Gyr	2.1	3.3	2.3	2.2	2.7	5.9	1.8
M_{vir} , 10^{10}	95	84	157	725	86	76	100
L_B , 10^{10}	3.3	6.8	6.1	6.0	2.5	3.2	2.7
M/L , solar	29	12	26	121	34	24	37

R_o , which separates the group from the global cosmic expansion, and then the total mass of the group defined by Lynden-Bell [14] as

$$M_t = (\pi^2/8G) \cdot R_o^3 \cdot T_o^{-2}.$$

Fig.6 exhibits the local Hubble flow in the immediate surroundings of the Local group. Distances and velocities are given with respect to the LG centroid. Similar "cold" velocity patterns are also seen around other nearest groups, yielding R_o values within 0.7 - 1.4 Mpc.

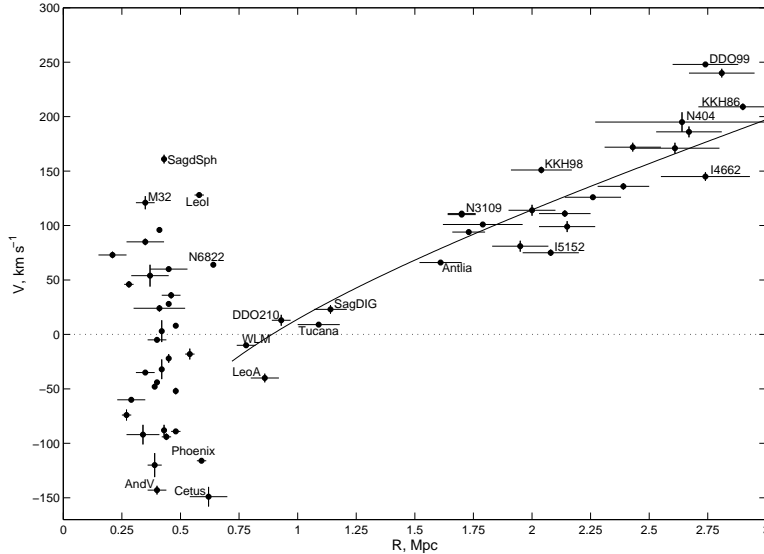


Fig. 6. The local Hubble flow in the immediate surroundings of the Local group

6 Some LV parameters important for cosmology.

In spite from the presence of local voids, the average density of luminosity within the radius of 8 Mpc around us exceeds 1.5 - 2.0 times the global luminosity density [6]. Almost the same excess is also seen in the local HI mass density [15]. About 2/3 of the LV galaxies belong to the known virialized groups like the LG. Because the average virial mass-to-luminosity ratio for them is $40 M_{\odot}/L_{\odot}$, the mean local mass density within 8 Mpc turns out to be 0.10 in units of the global critical density. This quantity is 2 - 3 times as low as the global density of matter, $\Omega_m = 0.27$. To remove the discrepancy between the global and local quantities of Ω_m , we assume that the essential amount of dark matter (70%) exists outside the virial radius of the groups.

It should be stressed that the number density of test particles (dwarf galaxies) in the LV is much higher than in any other distant volumes. Therefore, systematic investigating the LV has great advantage in probing the dark matter distribution on scales of 0.3 - 3 Mpc. In this respect we note that the sum of virial mass for 7 nearest groups (around the Milky Way, M 31, M81, CenA, M83, IC342, and Maffei) consists of $1.3 \cdot 10^{13} M_{\odot}$. But the sum of their total masses estimated via R_o from external galaxy motions is $0.86 \cdot 10^{13} M_{\odot}$ for the classical case $\Lambda = 0$, and $1.25 \cdot 10^{13} M_{\odot}$ for $\Omega_{\lambda} = 0.73$. Because the mean radius R_o for the groups exceeds 5 times their mean virial radius, the agreement of independent internal and external mass estimates may be interpreted as the

absence of a dark matter outside the R_{vir} . This unexpected result should be proven by new observational data.

Acknowledgements This work was supported by DFG–RFBR grant 06–02–04017 and RFBR grant 07-02-00005.

References

1. Kraan-Korteweg, R.C. & Tammann, G.A. 1979, AN, 300, 181
2. Karachentsev I.D., 1994, Astron. Astrophys. Trans., 6, 1
3. Staveley-Smith, L., Juraszek, S., Koribalski, B.S. et al. 1998, AJ, 116, 2717
4. Koribalski B.S. et al. 2004, AJ, 128, 16
5. Begum A., Chengalur J., Karachentsev I.D., et al. 2006, MNRAS, 365, 1220
6. Karachentsev I.D., Karachentseva V.E., Huchtmeier W.K., Makarov D.I., 2004, AJ, 127, 2031
7. Karachentsev I.D., 2005, AJ, 129, 178
8. Tikhonov, A.V. & Karachentsev, I.D. 2006, ApJ, 653, 969
9. Tully, R.B., Shaya E.J., Karachentsev I.D. et al. 2007, (astro-ph/0705.4139)
10. Carrasco L., Roth M., Serrano A., 1982, A&A, 106, 89
11. Roberts, M.S. 1969, AJ, 74, 859
12. Zasov, A.V. 1974, Astron. Zh., 51, 1225
13. Tutukov A.V., 2006, Astron. Rep., 50 526
14. Lynden-Bell D., 1981, Observatory, 101, 111
15. Zwaan, M.A., Staveley-Smith, L., Koribalski, B.S. et al. 2003, AJ, 125, 2842